Combined Effects of CO_2 and Light on the N_2-Fixing Cyanobacterium *Trichodesmium* IMS101: Physiological Responses[1][OA]

Sven A. Kranz*, Orly Levitan, Klaus-Uwe Richter, Ondřej Prášil, Ilana Berman-Frank, and Björn Rost

Alfred Wegener Institute for Polar and Marine Research, 27570 Bremerhaven, Germany (S.A.K., K.-U.R., B.R.); The Mina and Everard Goodman Faculty of Life Sciences, Bar Ilan University, Ramat-Gan, 52900 Israel (O.L., I.B.-F.); and Laboratory of Photosynthesis, Institute of Microbiology, Academy of Sciences of the Czech Republic, 37981 Třeboň, Czech Republic (O.P.)

Recent studies on the diazotrophic cyanobacterium *Trichodesmium erythraeum* (IMS101) showed that increasing CO_2 partial pressure (pCO_2) enhances N_2 fixation and growth. Significant uncertainties remain as to the degree of the sensitivity to pCO_2, its modification by other environmental factors, and underlying processes causing these responses. To address these questions, we examined the responses of *Trichodesmium* IMS101 grown under a matrix of low and high levels of pCO_2 (150 and 900 μatm) and irradiance (50 and 200 μmol photons m^{-2} s^{-1}). Growth rates as well as cellular carbon and nitrogen contents increased with increasing pCO_2 and light levels in the cultures. The pCO_2-dependent stimulation in organic carbon and nitrogen production was highest under low light. High pCO_2 stimulated rates of N_2 fixation and prolonged the duration, while high light affected maximum rates only. Gross photosynthesis increased with light but did not change with pCO_2. HCO_3^- was identified as the predominant carbon source taken up in all treatments. Inorganic carbon uptake increased with light, but only gross CO_2 uptake was enhanced under high pCO_2. A comparison between carbon fluxes in vivo and those derived from ^{13}C fractionation indicates high internal carbon cycling, especially in the low-pCO_2 treatment under high light. Light-dependent oxygen uptake was only detected under low pCO_2 combined with high light or when low-light-acclimated cells were exposed to high light, indicating that the Mehler reaction functions also as a photoprotective mechanism in *Trichodesmium*. Our data confirm the pronounced pCO_2 effect on N_2 fixation and growth in *Trichodesmium* and further show a strong modulation of these effects by light intensity. We attribute these responses to changes in the allocation of photosynthetic energy between carbon acquisition and the assimilation of carbon and nitrogen under elevated pCO_2. These findings are supported by a complementary study looking at photosynthetic fluorescence parameters of photosystem II, photosynthetic unit stoichiometry (photosystem I:photosystem II), and pool sizes of key proteins in carbon and nitrogen acquisition.

Human-induced climate change will significantly alter the marine environment within the next century and beyond. Future scenarios predict an increase from currently approximately 380 to about 750 to 1,000 μatm CO_2 partial pressure (pCO_2) in the atmosphere until the end of this century (Raven et al., 2005; Raupach et al., 2007). As the ocean takes up this anthropogenic CO_2, dissolved inorganic carbon (DIC) in the surface ocean increases while the pH decreases (Wolf-Gladrow et al., 1999). Rising global temperatures will increase surface ocean stratification, which may affect the light regime in the upper mixed layer as well as nutrient input from deeper waters (Doney, 2006). Uncertainties remain regarding both the magnitude of the physicochemical changes and the biological responses of organisms, including species and populations of the oceanic primary producers at the basis of the food webs.

In view of potential ecological implications and feedbacks on climate, several studies have examined pCO_2 sensitivity in phytoplankton key species (Burkhardt and Riebesell, 1997; Riebesell et al., 2000; Rost et al., 2003; Tortell et al., 2008). Pronounced responses to elevated pCO_2 were observed in N_2-fixing cyanobacteria (Barcelos é Ramos et al., 2007; Hutchins et al., 2007; Levitan et al., 2007; Fu et al., 2008; Kranz et al., 2009), which play a vital role in marine ecosystems by providing a new source of biologically available nitrogen species to otherwise nitrogen-limited regions. Recent studies focused on the impact of different environmental factors on the filamentous *Trichodesmium* species, which is

[1] This work was supported by the European Research Council under the European Community's Seventh Framework Programme (FP7/2007–2013)/ERC grant agreement (205150; to B.R.), by the Deutscher Akademischer Austausch Dienst (to O.L.), by the Czech Science Foundation-Grantová agentura České republiky (grant nos. 206/08/1683 and AV0Z50200510 to O.P.), by the Bundesministerium für Bildung und Forschung-Ministry of Science, Culture and Sport (grant no. GR1950 to I.B.-F.), and by a Ministry of Science, Culture and Sport Fellowship (to O.L.).

* Corresponding author; e-mail sven.kranz@awi.de.

The author responsible for distribution of materials integral to the findings presented in this article in accordance with the policy described in the Instructions for Authors (www.plantphysiol.org) is: Sven A. Kranz (sven.kranz@awi.de).

[OA] Open Access articles can be viewed online without a subscription.

www.plantphysiol.org/cgi/doi/10.1104/pp.110.159145

known for high abundance and the formation of massive blooms in tropical and subtropical areas (Capone et al., 2005; Mahaffey et al., 2005). Higher pCO_2 levels stimulated growth rates, biomass production, and N_2 fixation (Hutchins et al., 2007; Levitan et al., 2007; Kranz et al., 2009) and affected inorganic carbon acquisition of the cells (Kranz et al., 2009). While elevated sea surface temperatures are predicted to shift the spatial distribution of *Trichodesmium* species toward higher latitudes (Breitbarth et al., 2007), the combined effects of pCO_2 and temperature may favor this species and extend its niche even farther (Hutchins et al., 2007; Levitan et al., 2010a). An increase in the average light intensity, caused by the predicted shoaling of the upper mixed layer, may further stimulate photosynthesis and thus growth and N_2 fixation of *Trichodesmium* (Breitbarth et al., 2008). To our knowledge, the combined effects of light and pCO_2 have not been studied yet, although these environmental factors are likely to influence photosynthesis and other key processes in *Trichodesmium*.

To understand the responses of an organism to changes in environmental conditions, metabolic processes must be studied. In *Trichodesmium*, photosynthetically generated energy (ATP and NADPH) is primarily used for the fixation of CO_2 in the Calvin-Benson cycle. A large proportion of this energy, however, is also required for the process of N_2 fixation via nitrogenase and for the operation of a CO_2-concentrating mechanism (CCM). The latter involves active uptake of inorganic carbon, which functions to increase the rate of carboxylation reaction mediated by Rubisco. This ancient and highly conserved enzyme is characterized by low affinities for its substrate CO_2 and a susceptibility to a competing reaction with oxygen (O_2) as substrate (Badger et al., 1998); the latter initiates photorespiration. As cyanobacterial Rubisco possesses one of the lowest CO_2 affinities among phytoplankton (Badger et al., 1998), a considerable amount of resources have to be invested to achieve sufficient rates of carbon fixation and to avoid photorespiration. A first step toward a mechanistic understanding of responses in *Trichodesmium* has been taken by Levitan et al. (2007), focusing on pCO_2 dependency of nitrogenase activity and photosynthesis. Subsequently, Kranz et al. (2009) described variations in CCM efficiency with pCO_2 and suggested that the observed plasticity in CCM regulation allowed energy reallocation under high pCO_2, which may explain the observed pCO_2-dependent changes in nitrogenase activity, growth, and elemental composition (Barcelos é Ramos et al., 2007; Hutchins et al., 2007; Levitan et al., 2007).

In this study, we measured growth responses as well as metabolic key processes in *Trichodesmium erythraeum* (IMS101) under environmental conditions that likely alter the energy budget and/or energy allocation of the cell. Cultures were acclimated to a matrix of low and high pCO_2 (150 and 900 μatm) at two different light intensities (50 and 200 μmol photons m^{-2} s^{-1}). For each of the four treatments, changes in growth rates, elemental ratios, and the accumulation of particulate carbon and nitrogen were measured. Metabolic processes (gross photosynthesis, CCM activity, and O_2 uptake) were obtained by means of membrane-inlet mass spectrometry (MIMS), while N_2 fixation was detected by gas chromatography. As these processes may vary over the diurnal cycle in *Trichodesmium* (Berman-Frank et al., 2001; Kranz et al., 2009), measurements were performed in the morning and around midday. The results on metabolic processes were accompanied by measurements of the fluorescence of PSII, ratios of the photosynthetic units (PSI:PSII), and pool sizes of key proteins involved in carbon and nitrogen fixation as well as assimilation (Levitan et al., 2010b).

RESULTS

Elemental Composition, and Growth and Production Rates

Cellular quotas of particulate organic carbon (POC) and particulate organic nitrogen (PON) increased with both pCO_2 and light, while particulate phosphorus (PP) quotas remained constant in all treatments (one-way ANOVA for PP; $P > 0.05$; Table I). POC quota ranged between 3.79 ± 0.09 and 4.51 ± 0.21 pmol $cell^{-1}$ under low light and 4.60 ± 0.46 and 5.02 ± 0.57 pmol $cell^{-1}$ under high light (Table I). Elevated pCO_2 significantly increased the POC $cell^{-1}$ by 19% at low light (*t* test; $P = 0.001$) and by 9% (although not significant) at high light (*t* test; $P = 0.226$). PON quotas exhibited similar patterns, with values ranging from 0.59 ± 0.03 to 0.88 ± 0.06 pmol $cell^{-1}$ under low light and 0.86 ± 0.08 to 1.04 ± 0.09 pmol $cell^{-1}$ under high light at low and high pCO_2, respectively (Table I). The pCO_2-dependent changes in the PON quota were even larger than those of the POC, with a significant increase by 47% under low light (*t* test; $P < 0.001$) and 21% under high light (*t* test; $P < 0.05$). Respective carbon-nitrogen ratios decreased from 6.41 ± 0.39 to 5.04 ± 0.15 under low light (one-way ANOVA followed by a posthoc test; $P < 0.05$) and from 5.25 ± 0.19 to 4.85 ± 0.10 under high light with increasing pCO_2 (one-way ANOVA followed by a posthoc test; $P = 0.09$; Table I). Chlorophyll *a* (chl *a*) $cell^{-1}$ did not differ significantly between treatments, excluding cells grown under low light and low pCO_2 (one-way ANOVA followed by a posthoc test; $P < 0.001$; Table I).

Growth increased significantly with both elevated pCO_2 and higher light (one-way ANOVA followed by a posthoc test; $P < 0.001$). There was no difference between growth rate estimates whether based on changes in cell densities, chl *a*, POC, or PON; thus, they are reported as mean values. Growth rates ranged between 0.15 ± 0.03 and 0.24 ± 0.03 d^{-1} at low light and from 0.38 ± 0.02 to 0.42 ± 0.02 d^{-1} at high light (Fig. 1A). Elevated pCO_2 increased growth rates by 60% under low light and by 11% under high light. Rates of POC production also increased significantly under elevated pCO_2 (*t* test; $P < 0.001$), ranging

Table I. *Elemental composition of Trichodesmium IMS101 under a matrix of pCO_2 and light*

Values represent means of triplicate cultures, sampled over several days, all within exponential phase. Errors are ±1 SD ($n > 10$).

Elemental Composition	Acclimation			
	Low Light (50 μmol Photons m^{-2} s^{-1})		High Light (200 μmol Photons m^{-2} s^{-1})	
	150 μatm pCO_2	900 μatm pCO_2	150 μatm pCO_2	900 μatm pCO_2
POC (pmol carbon $cell^{-1}$)[a]	3.79 ± 0.09	4.51 ± 0.21	4.60 ± 0.46	5.02 ± 0.57
PON (pmol nitrogen $cell^{-1}$)[a]	0.59 ± 0.03	0.88 ± 0.06	0.86 ± 0.08	1.04 ± 0.09
PP (fmol phosphorus $cell^{-1}$)	73 ± 9	78 ± 9	70 ± 14	71 ± 4
Chl *a* (pg $cell^{-1}$)[b]	0.47 ± 0.04	0.72 ± 0.05	0.67 ± 0.14	0.69 ± 0.08
Carbon:nitrogen (mol:mol)[c]	6.41 ± 0.39	5.04 ± 0.15	5.25 ± 0.19	4.85 ± 0.10

[a]*t* test: significant difference between high-light acclimations. [b]*t* test: significant difference between low-light acclimations. [c]One-way ANOVA: significant difference between all acclimations.

between 0.57 ± 0.11 and 1.10 ± 0.17 pmol carbon $cell^{-1}$ d^{-1} under low light and between 1.76 ± 0.26 and 2.12 ± 0.34 pmol carbon $cell^{-1}$ d^{-1} under high light (Fig. 1B). The PON production increased under elevated pCO_2 (*t* test; $P < 0.001$), ranging between 0.09 ± 0.02 and 0.21 ± 0.04 pmol nitrogen $cell^{-1}$ d^{-1} under low light and between 0.33 ± 0.05 and 0.44 ± 0.06 pmol nitrogen $cell^{-1}$ d^{-1} under high light (Fig. 1C). Notably, at low light, elevated pCO_2 caused the strongest relative increase in POC and PON production, being 93% and 133% higher than under low pCO_2, respectively.

N_2 Fixation

Both the diurnal pattern and the rates of N_2 fixation responded strongly to pCO_2 and light (Fig. 2). For the low-light acclimations, N_2 fixation peaked 3 h after the beginning of the photoperiod with maximum rates, which range between 1.61 ± 0.51 and 3.03 ± 0.56 μmol N_2 mg chl a^{-1} h^{-1} for low and high pCO_2, respectively. Under high light, both pCO_2 acclimations peaked about 5 h after the onset of light, and maximum rates were 15.45 ± 1.29 and 19.21 ± 6.48 μmol N_2 mg chl a^{-1} h^{-1} for the low and high pCO_2 treatments, respectively (Fig. 2A). Elevated pCO_2 increased maximum rates about 2-fold under low light, while maximum rates appear not to differ at high light. More prominently, under high light, elevated pCO_2 led to a prolonged phase with high N_2 fixation rates, which lasted until the end of the photoperiod. This pCO_2 effect on the diurnal cycle was also present but less pronounced under low light. No N_2 fixation occurred during the dark period in all acclimations. As a result of the higher fixation rates and the prolonged N_2 fixation under elevated pCO_2, the integrated diurnal values of N_2 fixation increased by 200% and 112% under low and high light, respectively (Fig. 2B).

Photosynthetic O_2 Evolution and O_2 Uptake

Gross O_2 evolution increased with light but was neither affected by pCO_2 nor varied among measurements performed between 2 to 3 h (AM) and 6 to 7 h (PM) after the beginning of the photoperiod (Fig. 3A; Table II). O_2 evolution ranged between 119 ± 22 and 156 ± 4 μmol O_2 mg chl a^{-1} h^{-1} at low light and between 432 ± 153 and 534 ± 51 μmol O_2 mg chl a^{-1} h^{-1} at high light (Fig. 3A; Table II). O_2 uptake in the light was present in all treatments (Fig. 3B), yet rates were, with one exception, similar to those determined in the dark (Table II). At 150 μatm pCO_2 and 200 μmol photons m^{-2} s^{-1}, O_2 uptake in the light significantly exceeded dark respiration by about 140% in the morning and by about 70% during midday (*t* test; $P < 0.001$; Table II). Light-dependent O_2 uptake was also induced when cells acclimated to 50 μmol photons m^{-2} s^{-1} were exposed to 200 μmol photons m^{-2} s^{-1} during the measurements, irrespective of the pCO_2 level of the acclimation (Table II). Such instantaneous effects were also observed in the gross O_2 evolution (i.e. low-light-acclimated cells exposed to high light yielded rates similar to cells that had been acclimated to high light).

Inorganic Carbon Acquisition and Leakage

HCO_3^- was the major inorganic carbon source taken up by *Trichodesmium* in all acclimations, while CO_2 contributed only a minor fraction. Rates of HCO_3^- uptake were affected by both light and pCO_2, ranging from 82 ± 19 to 121 ± 25 μmol HCO_3^- mg chl a^{-1} h^{-1} in low light and from 224 ± 30 to 287 ± 50 μmol HCO_3^- mg chl a^{-1} h^{-1} in high light at low and high pCO_2, respectively (Table III). Under low light, HCO_3^- uptake decreased slightly, although not significantly, when cultures were acclimated to high pCO_2 (one-way ANOVA followed by a posthoc test; $P > 0.05$). Under high light, HCO_3^- uptake remained relatively stable at both pCO_2 levels. Rates of gross CO_2 uptake were affected by both light and pCO_2, ranging between 10 ± 1 and 22 ± 10 μmol CO_2 mg chl a^{-1} h^{-1} in low light and between 59 ± 6 and 147 ± 31 μmol CO_2 mg chl a^{-1} h^{-1} at high light at low and high pCO_2, respectively (Table II). To illustrate the contribution of each carbon species to the total carbon uptake, the ratio of HCO_3^- uptake to gross CO_2 uptake is depicted in Figure 4. Ratios ranged between 2 and 10, reflecting that HCO_3^- was the major carbon species taken up in all treatments. The

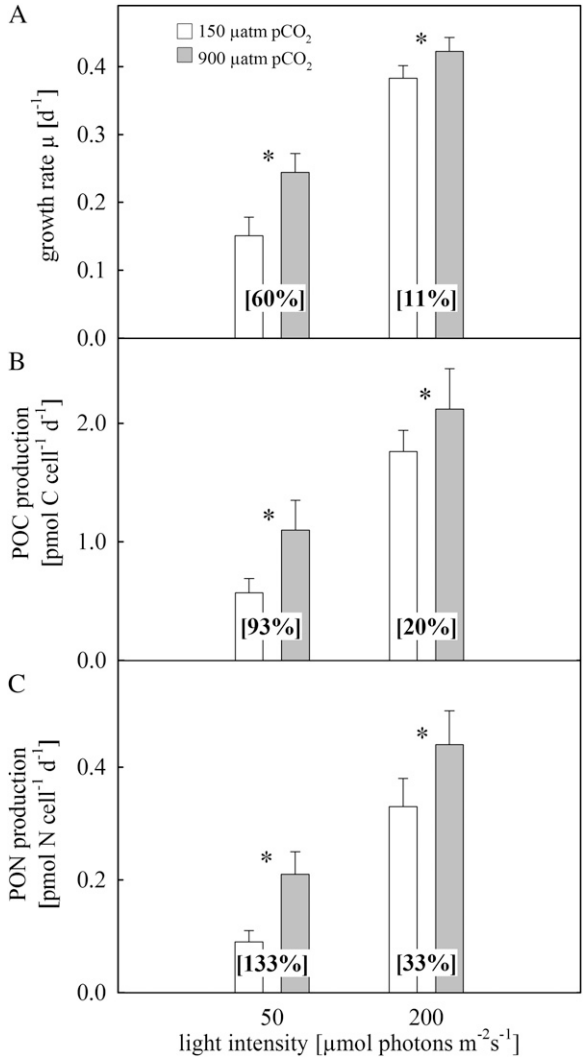

Figure 1. Responses of *Trichodesmium* IMS101 to different light (50 and 200 μmol photons m^{-2} s^{-1}) and pCO_2 (150 and 900 μatm) levels. A, Growth rates. B, Production rates of POC. C, Production rates of PON. Numbers in brackets denote the relative increase from low to high pCO_2 levels. Asterisks between bars indicate significant differences between low and high pCO_2 levels (*t* test; $P < 0.05$). Error bars indicate 1 SD ($n \geq 10$).

increased relevance of CO_2 uptake was indicated by the declining HCO_3^-:CO_2 uptake ratios under elevated pCO_2 and high light (Fig. 4). Rates of net O_2 evolution obtained in these assays (data not shown) were similar to those obtained in the assays on O_2 fluxes (Table II).

Cellular leakage (CO_2 efflux:gross carbon uptake) determined by MIMS measurements was generally low under low pCO_2, ranging between 0.24 ± 0.13 and 0.29 ± 0.19 in the low- and high-light acclimation, respectively (Table IV). In the high-pCO_2 acclimation, leakage was 0.41 ± 0.09 and 0.31 ± 0.14 in the low- and high-light acclimation, respectively. Leakage estimates deduced from ^{13}C fractionation were much higher than those measured directly by MIMS. In the low-pCO_2 acclimations, leakage was 0.57 ± 0.02 at high light and 0.84 ± 0.03 at low light, and it was about 0.90 in both high-pCO_2 acclimations (Table IV). These leakage estimates were derived from ^{13}C fractionation (ε_p), ranging between 12.94‰ ± 0.78‰ and 7.19‰ ± 0.58‰ under low pCO_2 at low and high light, respectively. Higher ε_p values were measured under elevated pCO_2, being 15.69‰ ± 1.12‰ and 16.54‰ ± 0.10‰ at low and high light, respectively.

DISCUSSION

The results of our study confirm the pronounced pCO_2 effect on N_2 fixation and growth in *Trichodesmium* and further show a strong modulation of these effects by irradiance. Cellular gas-exchange measurements revealed pCO_2-dependent changes in rates of N_2 fixation over the course of the photoperiod as well as in modes of carbon acquisition. Taken together, our

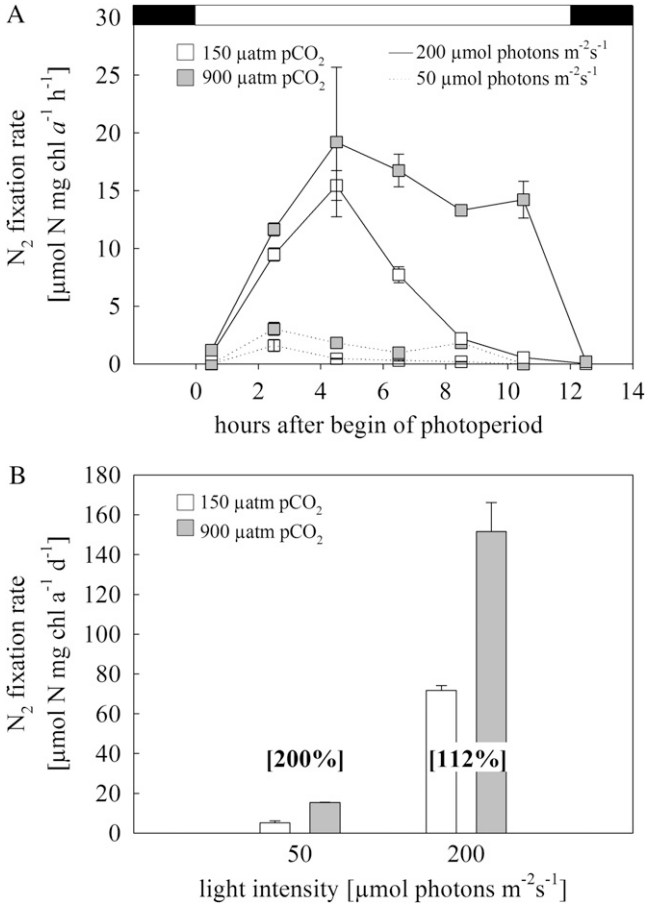

Figure 2. A, Diurnal cycle of nitrogen fixation of *Trichodesmium* IMS101 at the different light and pCO_2 acclimations. Measurements were obtained from duplicate cultures. Error bars indicate 1 SD. The black and white areas at top correspond to the dark and light periods of the diurnal cycle. B, Integrated diurnal N_2 fixation rate from A. Numbers in brackets denote the relative increase from low to high pCO_2 levels. Error bars indicate 1 SD ($n \geq 2$).

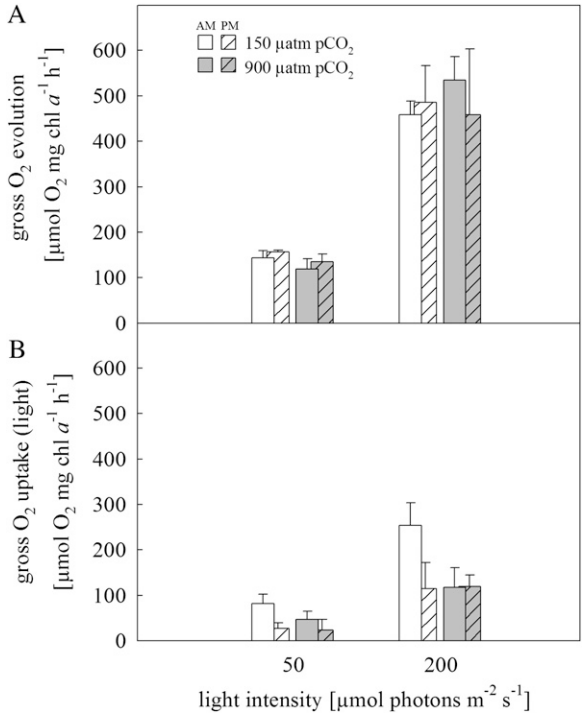

Figure 3. O_2 fluxes of *Trichodesmium* IMS101 measured between 2 to 3 h (AM; plain bars) and 6 to 7 h (PM; striped bars) after the beginning of the photoperiod. A, Gross O_2 evolution rate. B, Gross O_2 uptake rate in the light. Error bars indicate 1 SD ($n \geq 2$).

results indicate the reallocation of photosynthetic energy between both processes. Further evidence for this is presented in our complementary study (Levitan et al., 2010b).

Elemental Ratios, and Growth and Production Rates

Trichodesmium demonstrates high plasticity in growth and/or elemental composition with changing levels of pCO_2 (Barcelos é Ramos et al., 2007; Hutchins et al., 2007; Levitan et al., 2007; Kranz et al., 2009) and light (Breitbarth et al., 2008). The observed responses to these abiotic factors provide prima facie evidence for the increasing importance of *Trichodesmium* species in future oceans. In our study, the combined effect of pCO_2 and light, two factors that are predicted to change in the future ocean, were studied on *Trichodesmium* IMS101 and are discussed on an ecophysiological level.

The elemental composition of *Trichodesmium* cells showed an increase in POC and PON quotas with enhanced pCO_2 concentrations (Table I), a finding consistent with Kranz et al. (2009) but contradicting Barcelos é Ramos et al. (2007), who reported decreasing POC and PON quotas with elevated pCO_2. No pCO_2-dependent changes in elemental stoichiometry of carbon to nitrogen were observed in previous studies with light intensities between 80 and 150 μmol photons m^{-2} s^{-1} (Barcelos é Ramos et al., 2007; Hutchins et al., 2007; Levitan et al., 2007; Kranz et al., 2009). However, under 50 μmol photons m^{-2} s^{-1}, lower carbon-to-nitrogen ratios were obtained under elevated pCO_2 (Table I), reflecting a greater pCO_2 effect on the PON than on the POC quota under low light. Cell quotas for PP did not differ between acclimations (Table I), a finding that disagrees with decreasing organic phosphorus quotas under elevated pCO_2 observed by Barcelos é Ramos et al. (2007). The pCO_2-dependent increases in carbon-to-phosphorus and/or nitrogen-to-phosphorus ratios observed in this and previous studies imply that more biomass can be produced per available phosphorus.

The observed increase in growth rates under elevated pCO_2 (Fig. 1A) is consistent with previous findings from *Trichodesmium* (Barcelos é Ramos et al., 2007; Hutchins et al., 2007; Levitan et al., 2007). Yet, the magnitude in pCO_2-dependent stimulation differed strongly between studies and is probably associated with the different light intensities applied (approximately 80–150 μmol photons m^{-2} s^{-1}; Barcelos é Ramos et al., 2007; Hutchins et al., 2007; Levitan et al., 2007; Kranz et al., 2009). As our study focused

Table II. *O_2 fluxes in Trichodesmium IMS101 according to the method of Peltier and Thibault (1985)*

Values represent rates measured between 2 to 3 h (AM) and 6 to 7 h (PM) after the beginning of the photoperiod. Blanks denote no measurement. Errors are ±1 SD ($n \geq 3$). No SD is given when only one measurement was obtained.

Oxygen Fluxes	Assay Condition		Acclimation			
			Low Light (50 μmol Photons m^{-2} s^{-1})		High Light (200 μmol Photons m^{-2} s^{-1})	
			150 μatm pCO_2	900 μatm pCO_2	150 μatm pCO_2	900 μatm pCO_2
Gross O_2 evolution (μmol O_2 mg chl a^{-1} h^{-1})	Low light	AM	143 ± 16	119 ± 22		
		PM	156 ± 4	135 ± 17		
	High light	AM	453	538 ± 70	454 ± 28	534 ± 51
		PM	612	429 ± 42	486 ± 81	432 ± 153
O_2 uptake in the light (μmol O_2 mg chl a^{-1} h^{-1})	Low light	AM	81 ± 21	46 ± 18		
		PM	27 ± 12	23 ± 23		
	High light	AM	200	137 ± 33	254 ± 49	117 ± 42
		PM	81	83 ± 62	115 ± 57	123 ± 27
O_2 uptake in the dark (μmol O_2 mg chl a^{-1} h^{-1})	No light	AM	115 ± 10	83 ± 11	106 ± 44	126 ± 30
		PM	25 ± 8	24 ± 7	67 ± 13	111 ± 24

Table III. *Carbon fluxes in Trichodesmium IMS101 measured according to Badger et al. (1994)*
Values represent rates measured between 2 to 3 h (AM) and 6 to 7 h (PM) after the beginning of the photoperiod. Errors are ±1 SD ($n \geq 3$).

Inorganic Carbon Fluxes	Assay Condition		Acclimation			
			Low Light (50 μmol Photons m^{-2} s^{-1})		High Light (200 μmol Photons m^{-2} s^{-1})	
			150 μatm pCO_2	900 μatm pCO_2	150 μatm pCO_2	900 μatm pCO_2
Net fixation (μmol C mg chl a^{-1} h^{-1})	Same as acclimation	AM	98 ± 4	69 ± 7	301 ± 9	226 ± 55
		PM	92 ± 10	52 ± 8	330 ± 40	290 ± 15
HCO_3^- uptake (μmol HCO_3^- mg chl a^{-1} h^{-1})	Same as acclimation	AM	105 ± 8	82 ± 19	247 ± 50	224 ± 30
		PM	121 ± 25	98 ± 8	287 ± 50	282 ± 28
CO_2 uptake (μmol CO_2 mg chl a^{-1} h^{-1})	Same as acclimation	AM	10 ± 1	22 ± 10	59 ± 6	90 ± 19
		PM	17 ± 5	19 ± 6	61 ± 8	147 ± 31

on different pCO_2 levels in combination with low and high light, we could indeed verify that light levels strongly modify the responses of *Trichodesmium* to pCO_2 (Fig. 1; Table I). Like the responses in elemental composition, the relative changes in growth rates to elevated pCO_2 were largest under low light.

Due to the described effects on elemental composition and growth rates, the buildup of biomass in *Trichodesmium* increased strongly under elevated pCO_2 (Fig. 1, B and C). The pCO_2-dependent stimulation was highest under low light, with a 93% increase for POC production and a 133% increase for PON production relative to low pCO_2. Hutchins et al. (2007) measured ^{14}C incorporation over 24 h, an approach comparable to POC production rates in our study, and observed a 40% to 50% increase in carbon fixation when elevating the pCO_2 from 380 to 750 μatm pCO_2. Such responses in growth or POC production rates to elevated pCO_2 exceed those reported for other important marine phytoplankton groups such as diatoms and coccolithophores (Burkhardt et al., 1999; Zondervan et al., 2002; Langer et al., 2006) and demonstrate the exceptionally high sensitivity of *Trichodesmium* to pCO_2.

The strong responses in growth and POC and PON production rates corroborate previous publications stating that in *Trichodesmium*, central physiological processes must be pCO_2 sensitive. While processes like CCMs and carbon fixation are intrinsically CO_2 dependent (Giordano et al., 2005), a direct CO_2 effect on processes like N_2 fixation appeared unlikely. Furthermore, the observation that the pCO_2 sensitivity of POC and PON production rates is altered by light levels hints at an essential role of energy availability and allocation that we subsequently explored by measuring metabolic processes like N_2 fixation, gross photosynthetic O_2 evolution, CCM activity, as well as the Mehler reaction. Our complementary study focuses on these processes by measuring the respective protein pools (Levitan et al., 2010b).

N_2 Fixation

Since *Trichodesmium* cultures were grown in artificial medium without nitrogen sources and thus had to acquire all nitrogen for growth by fixation of dissolved N_2, the differences in PON production between treatments must be attributed to the respective changes in N_2 fixation. Under both low-light acclimations, N_2 fixation peaked about 3 h after onset of the light and showed reduced activities over midday until the end of the photoperiod (Fig. 2A). This atypical diurnal pattern may be caused by an energy shortage imposed by the low light levels, which first and foremost affect energy-demanding processes such as N_2 fixation. Despite energy shortage under low light, elevated pCO_2 highly stimulated N_2 fixation rates, which implies that more energy is available for this process. Under high light, maximum rates of N_2 fixation rates were more than 6-fold higher than in the low-light acclimations (Fig. 2A) and peaked during midday (5 h after onset of the light), as typically reported for *Trichodesmium* (Berman-Frank et al., 2001). While under low pCO_2, N_2 fixation rates declined after the midday peak, high pCO_2 levels resulted in a prolonged N_2 fixation until the end of the photoperiod. Such combined effects by light and pCO_2 on the diurnal patterns have not previously been reported and may indicate extended resource and energy availability for N_2 fixation and a

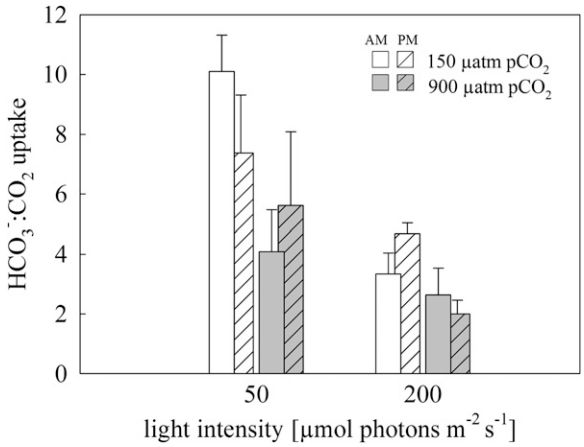

Figure 4. HCO_3^-:CO_2 uptake ratio in *Trichodesmium* IMS101 obtained from HCO_3^- and gross CO_2 uptake rates (Table III) measured between 2 to 3 h (AM; plain bars) and 6 to 7 h (PM; striped bars) after the beginning of the photoperiod. Error bars indicate 1 SD ($n \geq 3$).

Table IV. *Leakage (CO_2 efflux:gross carbon uptake) under respective culture conditions for Trichodesmium IMS101*
Values for two different approaches for leakage estimation are presented. Errors are ±1 SD ($n > 3$).

Approach	Acclimation			
	Low Light (50 μmol Photons m^{-2} s^{-1})		High Light (200 μmol Photons m^{-2} s^{-1})	
	150 μatm pCO_2	900 μatm pCO_2	150 μatm pCO_2	900 μatm pCO_2
MIMS-based leakage	0.24 ± 0.13	0.29 ± 0.19	0.41 ± 0.09	0.31 ± 0.14
^{13}C-based leakage	0.84 ± 0.03	0.92 ± 0.04	0.57 ± 0.02	0.90 ± 0.01

change in the regulation of nitrogenase (Levitan et al., 2010b).

As a consequence of the changes in rates and patterns of N_2 fixation under high light and elevated pCO_2, integrated N_2 fixation rates over the day increased by 200% under low light and 112% under high light (Fig. 2B). N_2 fixation by nitrogenase should be coupled to PON production (Fig. 1C), since N_2 is the only nitrogen source available. While both approaches indeed confirm the strong pCO_2 sensitivity in *Trichodesmium*, the relative stimulation by elevated pCO_2 was larger for the integrated N_2 fixation rates than those of the daily PON production (Figs. 1C and 2B). This apparent difference between acetylene reduction assay (i.e. gross N_2 fixation) and PON production (i.e. net N_2 fixation) could be explained by the loss of previously reduced N_2 as dissolved organic nitrogen (Capone et al., 1994; Glibert and Bronk, 1994) or ammonia (Mulholland et al., 2004) to the medium. In our experimental setup with continuous gas exchange, a significant proportion of ammonia may in fact be stripped out and subsequently cannot be used for PON production.

Fixation of N_2 and PON production differ in their demand for energy and resources. Consequently, pCO_2-dependent changes in the availability of energy and resources may affect both processes differently. While N_2 fixation by nitrogenase is mainly controlled by the availability of energy and electrons provided by the photosynthetic and respiratory pathways (a minimum of 16 ATP, eight electrons, and eight protons are required to reduce N_2 to NH_4^+), the PON accumulation is regulated by glutamine synthetase (GS) and glutamine oxoglutarate aminotransferase (GOGAT), called the GS/GOGAT pathway. The primary substrates for the GS/GOGAT pathway are NH_4^+ and α-ketoglutarate, a respiratory intermediate of the citric acid cycle, and this pathway requires relatively little energy (one ATP, one NADPH + H^+, and two protons to form one Glu). For a mechanistic understanding of these findings, it is important to look at possible regulations of key proteins in nitrogen metabolism (Levitan et al., 2010b).

What is the source of the additional energy and resources supporting the observed stimulation in N_2 fixation and PON production under elevated pCO_2? To answer this question, we compared the changes of energy generated in photosynthesis and energy consumed by processes involved in carbon metabolism.

Gross Photosynthesis

Photosynthesis generates energy and reductants that maintain metabolic processes such as N_2 fixation, carbon assimilation, and biomass buildup in *Trichodesmium*. In this study, direct measurements of gross photosynthesis (O_2 evolution from water splitting) yielded rates of photosynthetic electron generation, providing estimations about energy and reductant production. Regardless of pCO_2, gross photosynthesis was greatly stimulated by light (Fig. 3A). Thus, the enhanced N_2 fixation and PON production rates under high light (Figs. 1 and 2) can be explained by a higher supply of energy and reductants. Gross photosynthesis was insensitive to the applied pCO_2 levels (Fig. 3A). This is comparable with results obtained by Levitan et al. (2007), reporting no change in O_2 evolution for three different pCO_2 acclimations. The production of energy and reductants is not only set by electron generation at PSII but strongly controlled by the downstream processes along the electron transport chain. For example, rapid cyclic electron transport around PSI would yield higher ATP production at the expense of NADPH. We examined these light/pCO_2 effects in more detail at the level of the core proteins of PSII and PSI (Levitan et al., 2010b). Our findings show that elevated pCO_2 did not alter the supply of energy provided by gross photosynthesis. Thus, energy-demanding processes related to carbon metabolism must have been down-regulated to explain the strong stimulation in nitrogen metabolism under elevated pCO_2.

Inorganic Carbon Acquisition

Active acquisition of inorganic carbon is a mandatory process for the subsequent carbon fixation in the Calvin-Benson cycle. For the operation of these so-called CCMs, cyanobacteria like *Trichodesmium* need to invest a large amount of energy, which is primarily required due to the poor CO_2 affinity of Rubisco (Badger et al., 1998). *Trichodesmium* IMS101 operates an active CCM based predominantly on the uptake of HCO_3^- (Kranz et al., 2009). The relative HCO_3^- contribution to the total carbon fixation was about 90% and remained rather constant under all applied pCO_2 concentrations (150–1,000 μatm; Kranz et al., 2009). In this study, HCO_3^- was also the preferred carbon species in all treatments (Fig. 4; Table III). These results

concur with studies showing that CCMs in marine cyanobacteria are generally based on the transport and accumulation of HCO_3^- within the cell (Price et al., 2008). In some cyanobacteria, internal pools of inorganic carbon were up to 1,000-fold higher than ambient concentrations (Kaplan et al., 1980), emphasizing the generally high energetic costs of their CCMs.

Despite the predominance of HCO_3^- transport, gross CO_2 uptake rate increased under elevated pCO_2 (Fig. 4; Table III). Genome analysis identified the NAD(P)H dehydrogenase complex ($NDH1_4$), a CO_2 uptake system located at the thylakoid membrane (Ohkawa et al., 2001), to be present in *Trichodesmium*. This complex is considered to catalyze the conversion from CO_2 to HCO_3^- (Badger et al., 2006) by utilizing reductants or electrons provided mostly by electron transport (Friedrich and Scheide, 2000; Price et al., 2002, 2008) and may generate extra ATP by shuffling protons through the Q cycle of the thylakoid membrane (Friedrich and Scheide, 2000; Price et al., 2002). HCO_3^- uptake, on the other hand, is mediated by BicA transporters that are located in the plasma membrane and function as Na^+/HCO_3^- symporters (Price et al., 2004), which are indirectly energized by ATP hydrolysis. Consequently, the changes in HCO_3^- and CO_2 uptake observed in our study (Fig. 4) may reflect changes in the activity of the CCM components and the availability and/or utilization of ATP, NADPH, or reduced ferredoxin. Furthermore, the changes in uptake ratios may indicate a shift between linear and cyclic electron transport (Li and Canvin, 1998).

The energetic costs associated with the operation of a CCM (Raven and Lucas, 1985) play a central role in the overall energy budget of the cell. Kranz et al. (2009) observed a high plasticity of CCM regulation, for instance in DIC affinities, in response to changes in pCO_2 concentrations and over the photoperiod. Regulation of DIC affinities will likely alter the energy allocation between the CCM and other metabolic processes. The ability of *Trichodesmium* to down-regulate its DIC affinities under elevated pCO_2 (Kranz et al., 2009) and the observed up-regulation in the CO_2 uptake system (Fig. 4; Table III), therefore, could provide parts of the energetic "surplus" to explain the stimulation in nitrogen metabolism and/or organic carbon production.

Although the POC production rates increased significantly under elevated pCO_2 (Fig. 1B), rates of net carbon fixation in the MIMS assays were not stimulated in the high-pCO_2 treatment (Table III). Part of this apparent contradiction may result from the fact that POC production rates cover several generations, including dark and light phases, while net carbon fixation is based on "instantaneous" measurements at specific time points during the photoperiod. Such discrepancies between direct measurements of carbon fixation and daily POC turnover rates in *Trichodesmium* species were also reported for field populations (Mulholland et al., 2006). As *Trichodesmium* IMS101 was able to saturate carbon fixation in the assays at pCO_2 concentrations of the respective acclimations (data not shown; Kranz et al., 2009), we conclude that the observed changes in POC production cannot be caused by direct effects on the carboxylation efficiency of Rubisco but rather are due to changes in energy availability for downstream processes. Additional information on Rubisco quantities, energy requirements, and availability are provided by Levitan et al. (2010b).

Leakage and Internal Inorganic Carbon Cycling

In addition to the processes involved in inorganic carbon uptake and accumulation, the ability to reach high rates of carbon fixation also depends on the loss of inorganic carbon via leakage (CO_2 efflux:gross carbon uptake). MIMS-based estimates of leakage ranged between 0.24 and 0.41 in this study (Table IV), confirming values published previously for *Trichodesmium* (Kranz et al., 2009). Similar leakage estimates have been determined for other species of phytoplankton (Rost et al., 2006b; Trimborn et al., 2008), and such values seem reasonable for operating a cost-efficient CCM (Raven and Lucas, 1985). The leakage estimates obtained by ^{13}C fractionation, on the other hand, were found to be as high as 0.9 (Table IV), a value that would question the benefits of a CCM. It should be noted, however, that ^{13}C-based leakage estimates are dependent on several assumptions (e.g. the intrinsic fractionation of Rubisco). Also, this approach considers fluxes over the plasma membrane only. However, any kind of internal inorganic carbon cycling would increase ^{13}C fractionation as the accumulation of $^{13}CO_2$ at the site of carboxylation is lowered (Schulz et al., 2007). Following Sharkey and Berry (1985), high ^{13}C fractionation values caused by internal inorganic carbon cycling would then be misinterpreted as high leakage over the plasma membrane. Thus, the large differences between MIMS- and ^{13}C-based leakage estimates in our study likely reflect significant internal inorganic carbon cycling for *Trichodesmium*. High inorganic carbon cycling has also been indicated for other cyanobacteria based on exchange of ^{18}O from doubly labeled CO_2 in the light (Price et al., 2002, and refs. therein).

The NDH CO_2 uptake systems in cyanobacteria may be involved in both uptake of CO_2 and inorganic carbon cycling as a leakage prevention mechanism (Maeda et al., 2002; Price et al., 2002, 2008). The overestimation of ^{13}C-based leakage found in the high-pCO_2 treatments (Table IV) may thus reflect higher internal inorganic carbon cycling mediated by the $NDH1_4$ in *Trichodesmium*. Such inorganic carbon cycling appears consistent with the higher PSI-to-PSII ratio at elevated pCO_2 (Levitan et al., 2010b). An increasing role of $NDH1_4$ is also indicated by the higher gross CO_2 uptake rates under these conditions (Table III). As a consequence of higher inorganic carbon cycling, more ATP may be produced under elevated pCO_2 (Price et al., 2002), which in turn could

fuel the observed higher N_2 fixation (Fig. 2B). In the low-pCO_2 and high-light acclimation, the relatively small differences in leakage estimates indicate rather low internal inorganic carbon cycling (Table IV). This finding may be attributed to light-dependent O_2 uptake, which was observed only for this treatment (Fig. 3B; see "Discussion" below). Fluorescence data shown by Levitan et al. (2010b) also indicate low cyclic electron transport. However, further investigations on the dynamics of leakage and possible regulations by $NDH1_4$ in *Trichodesmium* have to be conducted to understand this essential process within its CCM.

Light-Dependent O_2 Uptake

Processes that reduce the O_2 concentration within the cell may play an important function in supporting and protecting nitrogenase in *Trichodesmium* from oxidative degradation (Kana, 1993; Berman-Frank et al., 2001; Milligan et al., 2007). In particular, the photoreduction of O_2 by the Mehler reaction catalyzes the conversion of O_2 to water. Changes in this O_2-scavenging process, therefore, could influence N_2 fixation rates. The Mehler reaction was also identified to be involved in photoprotection in other photoautotrophic species (Osmond and Grace, 1995; Osmond et al., 1997; Asada, 1999; Foyer and Noctor, 2000). To test for the presence and role of the Mehler reaction in our different acclimations, light-dependent O_2 uptake was measured.

In low-light-acclimated cells, in situ rates of O_2 uptake in the light were similar to the rates measured in the dark (Fig. 3B; Table II). Irrespective of the light treatment, the O_2 uptake rates were unaffected by the inhibition of PSII activity using 3-(3,4-dichlorophenyl)-1,1-dimethylurea (data not shown). Both observations indicate that the Mehler reaction was not present in *Trichodesmium* IMS101 grown under low light, regardless of pCO_2. Moreover, they indicate that the respiratory O_2 uptake via the terminal oxidase is not repressed during illumination. These findings provide an additional perspective to the current understanding of the Mehler reaction and the terminal oxidase activity in *Trichodesmium* (Milligan et al., 2007). It is likely that under the low light levels applied here, the Mehler reaction may not be beneficial, as it competes for the "scarce" electrons and its operation would decrease the energy supply for carbon and nitrogen fixation. In addition, the need for O_2 scavenging under low light is reduced because of low photosynthetic O_2 production relative to respiratory O_2 uptake (Table II).

In high-light-acclimated cells, the Mehler reaction was only detected under low pCO_2. Gross CO_2 uptake (i.e. $NDH1_4$ activity), inorganic carbon cycling, as well as nitrogenase activity were lower in this treatment than under high pCO_2. As these processes can use electrons supplied by ferredoxin, lower activities may enhance the proportion of reduced ferredoxin and impede electron transport. Under these conditions, the Mehler reaction could act as a shunt for routing excess electrons to avoid an overreduction and damage of PSII. Under elevated pCO_2, where the Mehler reaction was not observed, rates of gross CO_2 uptake, N_2 fixation, as well as POC and PON production may provide sufficient electron sinks, thereby reducing the need for the Mehler reaction.

Short-term exposure of the cells acclimated to 50 μmol photons m^{-2} s^{-1} to 200 μmol photons m^{-2} s^{-1} (6 min) resulted in a strong increase in light-dependent O_2 uptake, irrespective of the applied pCO_2 levels (Table II). The apparent operation of the Mehler reaction under these conditions may reduce the sudden electron flux within the electron transport chain, which otherwise may cause photodamage. Furthermore, the Mehler reaction may compensate for some of the light-stimulated O_2 evolution and thus act as a protection mechanism for nitrogenase. Such a relationship between the Mehler reaction and N_2 fixation was observed for *Trichodesmium* in several studies (Kana, 1993; Milligan et al., 2007). However, different growth conditions and the use of significantly higher light levels during these experiments (Kana, 1993; Milligan et al., 2007) could also account for the detection of the Mehler reaction in previous studies.

Under the conditions applied in this study, the Mehler reaction does not contribute to the observed stimulation in N_2 fixation under elevated pCO_2. Our findings suggest that under our experimental conditions, the Mehler reaction in *Trichodesmium* is involved in photoprotection rather than in O_2 scavenging. This proposed role may be advantageous in view of the high and variable light levels typical for the natural environments of *Trichodesmium* (La Roche and Breitbarth, 2005).

CONCLUSION

Our data on production rates and elemental composition bear important implications for future changes in the relevant biogeochemical cycles. The pCO_2-dependent stimulation in the rate of biomass production may increase the CO_2 drawdown in the upper mixed layer and affect the vertical transport of organic matter. This "fertilization" effect on *Trichodesmium* may also expand to other phytoplankton, as this important diazotroph fixes N_2 into particulate and dissolved compounds, thus providing a major source of bioavailable nitrogen to oligotrophic oceans

Table V. *Parameters of the seawater carbonate system*

Values were calculated from TA, pH, phosphate, temperature, and salinity using the CO2Sys program (Lewis and Wallace, 1998). Errors are ±1 SD ($n > 3$).

pCO_2	CO_2	TA	pH	DIC
μatm	*μmol kg^{-1}*	*μmol kg^{-1}*	*NBS*	*μmol kg^{-1}*
150	3.8 ± 0.3	2,487 ± 9	8.57 ± 0.03	1,841 ± 19
900	23.3 ± 1.5	2,470 ± 14	7.94 ± 0.03	2,240 ± 18

(Capone et al., 2005). In addition to the rate of production, biomass buildup is ultimately limited by the availability of other nutrients such as phosphorus. Consequently, the observed increase in carbon to phosphorus and/or nitrogen to phosphorus under elevated pCO_2 may imply that more biomass can be produced per available phosphorus, for instance over the course of a *Trichodesmium* bloom. In terms of the light-dependent changes in CO_2 sensitivity, the rise in pCO_2 may have a stronger effect on *Trichodesmium* thriving in deeper waters than for cells close to the surface. Furthermore, new information about metabolic key pathways and related proteins involved in carbon and nitrogen metabolism are provided in this and the complementary study (Levitan et al., 2010b). Although *Trichodesmium* can saturate carbon fixation even at low pCO_2 levels by operating an efficient CCM, this comes at an energetic cost and competes with other energy-demanding processes like N_2 fixation and the operation of the Calvin cycle. The observed responses to elevated pCO_2 could not be attributed to enhanced energy generation via gross photosynthesis. Instead, energetic costs of the CCM were reduced under high pCO_2, providing a surplus of energy and reductants that in turn enabled higher rates of N_2 fixation and PON and POC production and growth. Future studies should investigate whether phosphorus and iron limitation, often prevailing in oligotrophic waters, may modify the described effects of this study.

MATERIALS AND METHODS

Culture Conditions

Cultures of *Trichodesmium erythraeum* (strain IMS101; originally isolated by Prufert-Bebout et al., 1993) were grown at 25°C in 0.2-μm-filtered unbuffered nitrogen-free artificial seawater (YBCII medium; Chen et al., 1996). All cells were cultured as single filaments, grown in 1-L cylindrical glass flasks (diameter of 7 cm), and incubated in a light:dark cycle (12:12 h) with light provided by white fluorescent bulbs (Osram; BIOLUX) at two different light intensities (50 and 200 μmol photons m^{-2} s^{-1}), representing light-limiting and light-saturating values for *Trichodesmium* according to Breitbarth et al. (2008). Cultures were continuously bubbled with air containing different pCO_2 values of 150 and 900 μatm. The bubbling was sufficient to avoid aggregate formation but did not alter the integrity of the filaments. CO_2 gas mixtures were generated with gas-mixing pumps (Digamix 5KA18/8-F and 5KA36/8-F; Woesthoff) using CO_2-free air (Nitrox CO_2RP280; Domnick Hunter) and pure CO_2 (Air Liquide Deutschland). Dilute batch cultivation (i.e. regular dilution with fresh, preequilibrated medium) ensured that the carbonate chemistry remained constant and cells stayed in the midexponential growth phase. Cultures in which the pH shifted (pH shift > 0.06) in comparison with a reference (i.e. cell-free medium at the respective pCO_2 levels) were excluded from further analysis.

Seawater Carbonate Chemistry

Samples for total alkalinity (TA) were taken from the culture filtrate (Whatman GFF filter; approximately 0.6 μm), stored in 100-mL borosilicate bottles at room temperature, and measured by potentiometric titration (Brewer et al., 1981) with an average precision of ± 10 μmol kg^{-1}. TA was calculated from linear Gran Plots (Gran, 1952). TA measurements were calibrated with certified reference material (Dr. Andrew Dickson, Scripps Institution of Oceanography). The pH_{NBS} was determined every morning using a pH/ion meter (model 713 pH meter; Metrohm). The carbonate system was calculated from TA, pH_{NBS}, temperature, salinity, and phosphate using CO2Sys (Lewis and Wallace, 1998). Equilibrium constants of Mehrbach et al. (1973) refitted by Dickson and Millero (1987) were chosen. Carbonate chemistry for the respective pCO_2 treatments are given in Table V.

Elemental Composition, and Growth and Production Rates

Cells were acclimated to the respective pCO_2 and light levels for at least 30 d (more than 10 generations) prior to harvesting. In all acclimations, samples for growth responses were taken simultaneously at the beginning of the photoperiod to account for diurnal changes. Cell densities were determined using an inverted microscope (Zeiss Axiovert 200) by measuring the number and the length of filaments as well as the cell size in a Sedgwick-Rafter Cell (S50; Graticules).

Samples for POC, PON, and PP were filtered onto precombusted (500°C, 9 h) glass fiber filters (GF/F) and stored in precombusted (500°C, 9 h) petri dishes at −20°C. Prior to analysis, filters for POC were treated with 200 μL of HCl (0.1 N) to remove all inorganic carbon. POC and PON filters were measured in duplicate with a mass spectrometer (ANCA-SL 2020), with an average precision of ± 1 μg of carbon and ± 0.5 μg of nitrogen, respectively. PP was measured photometrically using a modified version of the ALOHA protocol (Hawaii Institute of Marine Biology, Analytical Services Laboratory at the University of Hawaii).

Growth and POC and PON production rates were determined based on changes in cell density, chl *a*, as well as POC and PON. Growth rates (μ) were calculated according to the following equation:

$$\mu\left[d^{-1}\right] = \frac{\ln(N_1) - \ln(N_0)}{\Delta t}$$

where N_0 and N_1 are concentrations (cell, chl *a*, POC, PON) at the beginning (t_o) and the end (t_1) of sampling, and Δt is the time between sampling intervals. Production rates of POC and PON were calculated according to the following equations:

$$\text{POC production} = \mu \times \text{POC cell}^{-1}$$

$$\text{PON production} = \mu \times \text{PON cell}^{-1}$$

Samples for chl *a* were filtered on GF/filters and immediately stored at −80°C. Chl *a* was subsequently extracted in 5 to 10 mL of 90% acetone (overnight in darkness at 4°C) and determined with a fluorometer (Turner Designs) by measuring nonacidified and acidified fluorescence.

N_2 Fixation

Rates of N_2 fixation were estimated using the acetylene reduction assay (Capone, 1993). The samples (concentrations between 0.02 and 0.08 μg chl *a* mL^{-1}) were spiked with acetylene (20% of head space volume) and incubated for 1 h at acclimation light and temperature with gentle continuous shaking of the bottles to avoid aggregation or settlement. The rate of acetylene reduction to ethylene was measured using a gas chromatograph with a flame-ionization detector (Thermo Finnigan Trace) and quantified relative to an ethylene standard. Rates were normalized to chl *a*, and a conversion factor of 4:1 (Capone and Montoya, 2001) was applied to convert ethylene production to N_2 fixation rates. To account for the diurnal patterns, nitrogen fixation rates were measured every 2 h from the onset of light until 2 h after dark.

Photosynthetic O_2 Evolution and O_2 Uptake

Rates of net O_2 production and O_2 uptake were measured by MIMS. All MIMS measurements were carried out in an 8-mL thermostatted cuvette, which was attached to a sectorfield multicollector mass spectrometer (Isoprime; GV Instruments) via a gas-permeable membrane (PTFE; 0.01 mm) inlet system. O_2-evolving and O_2-consuming processes can be separated in the light by measuring $^{16}O_2$ evolution from water splitting and $^{18}O_2$ uptake from the medium. To this end, the medium was initially bubbled with nitrogen to remove all the $^{16}O_2$ and then enriched with $^{18}O_2$, ensuring that mainly $^{18}O_2$ is taken up by O_2-consuming processes. For further details on the calculations of

O_2 fluxes, the reader is referred to Peltier and Thibault (1985) and Fock and Sültemeyer (1989).

Assays were performed in YBCII medium buffered with HEPES (50 mM, pH 7.8) or Bicine (50 mM, pH 8.4) depending on the respective pCO_2 of the acclimation. To obtain assay conditions, the medium was purged with N_2 overnight, subsequently sealed in 40-mL glass bottles, and spiked with 20 to 40 μL of $^{18}O_2$ to yield air-equilibrated O_2 concentrations (i.e. 21%). For measurements, cells were concentrated by gentle filtration (8 μm; Isopore; Millipore). The culture medium was exchanged stepwise with the $^{18}O_2$-enriched assay medium, and cells were subsequently transferred to the MIMS cuvette. Light and dark intervals lasted 6 min to obtain O_2 fluxes under steady-state conditions. DIC concentrations were adjusted by the addition of a 1 M HCO_3^- solution prior to measurements. Measurements were performed at respective acclimation light (50 or 200 μmol photons m^{-2} s^{-1}) and DIC (approximately 1,900 or 2,300 μmol of DIC) levels if not mentioned otherwise. Chl *a* concentration during the measurement ranged between 0.4 and 1.6 μg mL^{-1}.

Inorganic Carbon Acquisition and Leakage

Uptake of net photosynthesis, inorganic carbon sources (CO_2 or HCO_3^-) for photosynthesis, and leakage (CO_2 efflux:gross carbon uptake) were determined by MIMS measurements according to Badger et al. (1994). This approach is based on simultaneous measurements of O_2 and CO_2 during consecutive light and dark intervals at steady-state photosynthesis. For measurements, cells were concentrated in the same manner as for the O_2 flux measurements, exchanging growth medium with assay medium (pH 7.8 and 8.4) containing air-equilibrated O_2 levels. Light and dark intervals during the assay lasted 6 min. Light was adjusted to the respective photon flux densities in the acclimation (50 or 200 μmol photons m^{-2} s^{-1}). To completely inhibit external carbonic anhydrase activity, dextran-bound sulfonamide was added to a final concentration of 50 μmol L^{-1}. Chl *a* concentrations during the measurement ranged between 0.5 and 2 μg mL^{-1}. Further details on the method and calculations are given by Badger et al. (1994) and Rost et al. (2007).

To obtain additional information about leakage, isotopic composition of POC ($\delta^{13}C_{POC}$) was determined by EA-mass spectrometry (ANCA-SL 2020) following Rost et al. (2006a). Isotopic fractionation during POC formation (ε_p) was calculated relative to the isotopic composition of CO_2 ($\delta^{13}C_{CO2}$) in the medium. To determine the isotopic composition of DIC ($\delta^{13}C_{DIC}$), 8 mL of the culture medium was fixed with $HgCl_2$ (approximately 110 mg L^{-1} final concentration). Extractions and measurements were performed in the laboratory of H.J. Spero (University of California, Davis) with a precision of ± 0.11‰. The isotopic composition of CO_2 ($\delta^{13}C_{CO2}$) was calculated from $\delta^{13}C_{DIC}$, following a mass-balance equation (Zeebe and Wolf-Gladrow, 2007). Isotopic fractionation is driven by the intrinsic discrimination of ^{13}C by Rubisco (ε_f), setting the upper-most values for ε_P. Variations in fractionation are principally determined by changes in leakage as well as carbon source taken up (Sharkey and Berry, 1985):

$$\varepsilon_P = a \times \varepsilon_s + L \times \varepsilon_f$$

where ε_f is assumed to be approximately 25‰ (Guy et al., 1993), ε_s represents the equilibrium fractionation between CO_2 and HCO_3^-, and *a* is the fractional contribution of HCO_3^- to total inorganic carbon uptake. Since HCO_3^- is about 9‰ enriched in ^{13}C relative to CO_2 (Zeebe and Wolf-Gladrow, 2007), an increasing proportion of HCO_3^- uptake reduces the ε_P value, which is defined relative to CO_2 as the carbon source. If there is no change in carbon source, ε_P increases with increasing leakage.

ACKNOWLEDGMENTS

We thank Torben Genz for technical support and two anonymous reviewers for their constructive comments on the manuscript.

Received May 13, 2010; accepted July 11, 2010; published July 12, 2010.

LITERATURE CITED

Asada K (1999) The water-water cycle in chloroplasts: scavenging of active oxygens and dissipation of excess photons. Annu Rev Plant Physiol Plant Mol Biol **50:** 601–639

Badger MR, Andrews TJ, Whitney SM, Ludwig M, Yellowlees DC (1998) The diversity and co-evolution of Rubisco, plastids, pyrenoids and chloroplast-based CO_2-concentrating mechanisms in the algae. Can J Bot **76:** 1052–1071

Badger MR, Palmqvist K, Yu JW (1994) Measurement of CO_2 and HCO_3^- fluxes in cyanobacteria and microalgae during steady-state photosynthesis. Physiol Plant **90:** 529–536

Badger MR, Price GD, Long BM, Woodger FJ (2006) The environmental plasticity and ecological genomics of the cyanobacterial CO_2 concentrating mechanism. J Exp Bot **57:** 249–265

Barcelos é Ramos J, Biswas H, Schulz KG, LaRoche J, Riebesell U (2007) Effect of rising atmospheric carbon dioxide on the marine nitrogen fixer *Trichodesmium*. Global Biogeochem Cycles **21:** doi/10.1029/2006GB002898

Berman-Frank I, Lundgren P, Chen YB, Küpper H, Kolber Z, Bergman B, Falkowski P (2001) Segregation of nitrogen fixation and oxygenic photosynthesis in the marine cyanobacterium *Trichodesmium*. Science **294:** 1534–1537

Breitbarth E, Oschlies A, LaRoche J (2007) Physiological constraints on the global distribution of *Trichodesmium*: effect of temperature on diazotrophy. Biogeosciences **4:** 53–61

Breitbarth E, Wohlers J, Kläs J, LaRoche J, Peeken I (2008) Nitrogen fixation and growth rates of *Trichodesmium* IMS-101 as a function of light intensity. Mar Ecol Prog Ser **359:** 25–36

Brewer PG, Bradshaw AL, Williams RT (1981) Measurements of total carbon dioxide and alkalinity in the North Atlantic Ocean. *In* JR Trabalka, DE Reichle, eds, The Changing Carbon Cycle: A Global Analysis. Springer, New York, pp 348–370

Burkhardt S, Riebesell U (1997) CO_2 availability affects elemental composition (C:N:P) of the marine diatom *Skeletonema costatum*. Mar Ecol Prog Ser **155:** 67–76

Burkhardt S, Riebesell U, Zondervan I (1999) Stable carbon isotope fractionation by marine phytoplankton in response to daylength, growth rate, and CO_2 availability. Mar Ecol Prog Ser **184:** 31–41

Capone DG (1993) Determination of nitrogenase activity in aquatic samples using the acetylene reduction procedure. *In* PF Kemp, B Sherr, E Sherr, J Cole, eds, Handbook of Methods in Aquatic Microbial Ecology. Lewis Publishers, New York, pp 621–631

Capone DG, Burns JA, Montoya JP, Subramaniam A, Mahaffey C, Gunderson T, Michaels AF, Carpenter EJ (2005) Nitrogen fixation by *Trichodesmium* spp.: an important source of new nitrogen to the tropical and subtropical North Atlantic Ocean. Global Biogeochem Cycles **19:** GB2024, 10.1029/2004GB002331

Capone DG, Ferrier MD, Carpenter EJ (1994) Cycling and release of glutamate and glutamine in colonies of the marine planktonic cyanobacterium, *Trichodesmium thiebautii*. Appl Environ Microbiol **60:** 3989–3995

Capone DG, Montoya JP (2001) Nitrogen fixation and denitrification. Methods Microbiol **30:** 501–515

Chen YB, Zehr JP, Mellon M (1996) Growth and nitrogen fixation of the diazotrophic filamentous nonheterocystous cyanobacterium *Trichodesmium* sp. IMS 101 in defined media: evidence for a circadian rhythm. J Phycol **32:** 916–923

Dickson AG, Millero FJ (1987) A comparison of the equilibrium constants for the dissociation of carbonic acid in seawater media. Deep Sea Res **34:** 1733–1743

Doney SC (2006) Oceanography: plankton in a warmer world. Nature **444:** 695–696

Fock HP, Sültemeyer DF (1989) O_2 evolution and uptake measurements in plant cells by mass spectrometer. *In* HF Liskens, JF Jackson, eds, Modern Methods of Plant Analysis, Vol 9. Springer-Verlag, Heidelberg, pp 3–18

Foyer CH, Noctor G (2000) Oxygen processing in photosynthesis: regulation and signaling. New Phytol **146:** 359–388

Friedrich T, Scheide D (2000) The respiratory complex I of bacteria, archaea and eukarya and its module common with membrane-bound multisubunit hydrogenases. FEBS Lett **497:** 1–5

Fu FX, Mulholland MR, Garcia NS, Beck A, Bernhardt PW, Warner ME, Sanudo-Wilhelmy SA, Hutchins DA (2008) Interactions between changing pCO_2, N_2 fixation, and Fe limitation in the marine unicellular cyanobacterium *Crocosphaera*. Limnol Oceanogr **53:** 2472–2484

Giordano M, Beardall J, Raven JA (2005) CO_2 concentrating mechanisms in algae: mechanisms, environmental modulation, and evolution. Annu Rev Plant Biol **56:** 99–131

Glibert PM, Bronk DA (1994) Release of dissolved organic nitrogen by

marine diazotrophic cyanobacteria, *Trichodesmium* spp. Appl Environ Microbiol **60:** 3996–4000

Gran G (1952) Determination of the equivalence point in potentiometric titrations. Part II. Analyst (Lond) **77:** 661–671

Guy RD, Fogel ML, Berry JA (1993) Photosynthetic fractionation of stable isotopes of oxygen and carbon. Plant Physiol **101:** 37–47

Hutchins DA, Fu FX, Zhang Y, Warner ME, Feng Y, Portune K, Bernhardt PW, Mulholland MR (2007) CO_2 control of *Trichodesmium* N_2 fixation, photosynthesis, growth rates and elemental ratios: implications for past, present and future ocean biogeochemistry. Limnol Oceanogr **552:** 1293–1304

Kana TM (1993) Rapid oxygen cycling in *Trichodesmium thiebautii*. Limnol Oceanogr **38:** 18–24

Kaplan A, Badger MR, Berry JA (1980) Photosynthesis and the intracellular inorganic carbon pool in the blue green alga *Anabaena variabilis*: response to external CO_2 concentration. Planta **149:** 219–226

Kranz SA, Sültemeyer D, Richter KU, Rost B (2009) Carbon acquisition in *Trichodesmium*: the effect of pCO_2 and diurnal changes. Limnol Oceanogr **54:** 548–559

Langer G, Geisen M, Baumann KH, Kläs J, Riebesell U, Thoms S, Young JR (2006) Species-specific responses of calcifying algae to changing seawater carbonate chemistry. Geochemistry Geophysics Geosystems **7:** Q09006

La Roche J, Breitbarth E (2005) Importance of the diazotrophs as a source of new nitrogen in the ocean. J Sea Res **53:** 67–91

Levitan O, Brown CM, Sudhaus S, Campbell D, LaRoche J, Berman-Frank I (2010a) Regulation of nitrogen metabolism in the marine diazotroph *Trichodesmium* IMS101 under varying temperatures and atmospheric CO_2 concentrations. Environ Microbiol **12:** 1899–1912

Levitan O, Kranz SA, Spungin D, Prášil O, Rost B, Berman-Frank I (2010b) Combined effects of CO_2 and light on the N_2-fixing cyanobacterium *Trichodesmium* IMS101: a mechanistic view. Plant Physiol **154:** 346–356

Levitan O, Rosenberg G, Setlik I, Setlikova E, Grigel J, Klepetar J, Prášil O, Berman-Frank I (2007) Elevated CO_2 enhances nitrogen fixation and growth in the marine cyanobacterium *Trichodesmium*. Glob Change Biol **13:** 531–538

Lewis E, Wallace DWR (1998) Program developed for CO_2 system calculations. ORNL/CDIAC-105. Carbon Dioxide Information Analysis Center, Oak Ridge National Laboratory, U.S. Department of Energy, Oak Ridge, TN

Li QL, Canvin DT (1998) Energy sources for HCO_3^- and CO_2 transport in air-grown cells of *Synechococcus* UTEX 625. Plant Physiol **116:** 1125–1132

Maeda S, Badger MR, Price GD (2002) Novel gene products associated with NdhD3/D4-containing NDH-1 complexes are involved in photosynthetic CO_2 hydration in the cyanobacterium *Synechococcus* sp. PCC7942. Mol Microbiol **43:** 425–435

Mahaffey C, Michaels AF, Capone DG (2005) The conundrum of marine N_2 fixation. Am J Sci **305:** 546–595

Mehrbach C, Culberson CH, Hawley JE, Pytkowicz RM (1973) Measurement of the apparent dissociation constants of carbonic acid in seawater at atmospheric pressure. Limnol Oceanogr **18:** 897–907

Milligan AJ, Berman-Frank I, Gerchman Y, Dismukes GC, Falkowski PG (2007) Light-dependent oxygen consumption in nitrogen-fixing cyanobacteria plays a key role in nitrogenase protection. J Phycol **43:** 845–852

Mulholland MR, Bronk DA, Capone DG (2004) Dinitrogen fixation and release of ammonium and dissolved organic nitrogen by *Trichodesmium* IMS101. Aquat Microb Ecol **37:** 85–94

Mulholland MR, Heil CA, Bronk DA, O'Neil MO (2006) Nitrogen fixation and release of fixed nitrogen by *Trichodesmium* sp. in the Gulf of Mexico. Limnol Oceanogr **51:** 1762–1776

Ohkawa H, Sonoda M, Shibata M, Ogawa T (2001) Localization of NAD (P)H dehydrogenase in the cyanobacterium *Synechocystis* sp strain PCC 6803. J Bacteriol **183:** 4938–4939

Osmond CB, Badger MR, Maxwell K, Bjoerkman O, Leegood RC (1997) Too many photons: photorespiration, photoinhibition and photooxidation. Trends Plant Sci **2:** 119–121

Osmond CB, Grace SC (1995) Perspectives on photoinhibition and photorespiration in the field: quintessential inefficiencies of the light and dark reactions of photosynthesis? J Exp Bot **46:** 1351–1362

Peltier G, Thibault P (1985) O_2 uptake in the light in *Chlamydomonas*: evidence for persistent mitochondrial respiration. Plant Physiol Biochem **79:** 225–230

Price GD, Badger MR, Woodger FJ, Long BM (2008) Advances in understanding the cyanobacterial CO_2-concentrating-mechanism (CCM): functional components, Ci transporters, diversity, genetic regulation and prospects for engineering into plants. J Exp Bot **59:** 1441–1461

Price GD, Maeda SI, Omata T, Badger MR (2002) Modes of inorganic carbon uptake in the cyanobacterium *Synechococcus* sp. PCC7942. Funct Plant Biol **29:** 131–149

Price GD, Woodger FJ, Badger MR, Howitt SM, Tucker L (2004) Identification of a SulP-type bicarbonate transporter in marine cyanobacteria. Proc Natl Acad Sci USA **101:** 18228–18233

Prufert-Bebout L, Paerl HW, Lassen C (1993) Growth, nitrogen fixation, and spectral attenuation in cultivated *Trichodesmium* species. Appl Environ Microbiol **59:** 1367–1375

Raupach MR, Marland G, Ciais P, Le Quere C, Canadell JG, Klepper G, Field CB (2007) Global and regional drivers of accelerating CO_2 emissions. Proc Natl Acad Sci USA **104:** 10288–10293

Raven J, Caldeira K, Elderfield H, Hoeg-Guldberg O, Liss P, Riebesell U, Shepherd J, Turley C, Watson A (2005) Ocean Acidification Due to Increasing Atmospheric Carbon Dioxide. Policy Document 12/05. The Royal Society, London. Clyvedon Press Ltd., Cardiff, UK

Raven JA, Lucas WJ (1985) Energy costs of carbon acquisition. *In* WJ Lucas, JA Berry, eds, Inorganic Carbon Uptake by Aquatic Photosynthetic Organisms. American Society of Plant Physiologists, Rockville, MD, pp 305–324

Riebesell U, Zondervan I, Rost B, Tortell PD, Zeebe E, Morel FMM (2000) Reduced calcification in marine plankton in response to increased atmospheric CO_2. Nature **407:** 634–637

Rost B, Kranz SA, Richter KU, Tortell PD (2007) Isotope disequilibrium and mass spectrometric studies of inorganic carbon acquisition by phytoplankton. Limnol Oceanogr Methods **5:** 328–337

Rost B, Richter KU, Riebesell U, Hansen PJ (2006a) Inorganic carbon acquisition in red-tide dinoflagellates. Plant Cell Environ **29:** 810–822

Rost B, Riebesell U, Burkhardt S, Sültemeyer D (2003) Carbon acquisition of bloom-forming marine phytoplankton. Limnol Oceanogr **48:** 55–67

Rost B, Riebesell U, Sültemeyer D (2006b) Carbon acquisition of marine phytoplankton: effect of photoperiod length. Limnol Oceanogr **51:** 12–20

Schulz KG, Rost B, Burkhardt S, Riebesell U, Thoms S, Wolf-Gladrow DA (2007) The effect of iron availability on the regulation of inorganic carbon acquisition in the coccolithophore *Emiliania huxleyi* and the significance of cellular compartmentation for stable carbon isotope fractionation. Geochim Cosmochim Acta **71:** 5301–5312

Sharkey TD, Berry JA (1985) Carbon isotope fractionation of algae influenced by an inducible CO_2-concentrating mechanism. *In* WJ Lucas, JA Berry, eds, Inorganic Carbon Uptake by Aquatic Photosynthetic Organisms. American Society of Plant Physiologists, Rockville, MD, pp 389–401

Tortell PD, Payne CD, Li Y, Trimborn S, Rost B, Smith WO, Riesselman C, Dunbar R, Sedwick P, DiTullio G (2008) The CO_2 response of southern ocean phytoplankton. Geophys Res Lett **35:** L04605

Trimborn S, Lundholm N, Thoms S, Richter KU, Krock B, Hansen PJ, Rost B (2008) Inorganic carbon acquisition in potentially toxic and non-toxic diatoms: the effect of pH-induced changes in seawater carbonate chemistry. Physiol Plant **133:** 92–105

Wolf-Gladrow DA, Bijma J, Zeebe RE (1999) Model simulation of the carbonate chemistry in the microenvironment of symbiont bearing foraminifera. Mar Chem **64:** 181–198

Zeebe RE, Wolf-Gladrow DA (2007) CO_2 in Seawater: Equilibrium, Kinetics, Isotopes. Elsevier Science, Amsterdam

Zondervan I, Rost B, Riebesell U (2002) Effect of CO_2 concentration on the PIC/POC ratio in the coccolithophore *Emiliania huxleyi* grown under light-limiting conditions and different daylengths. J Exp Mar Biol Ecol **272:** 55–70